THE JOURNAL OF BIOLOGICAL CHEMISTRY VOL. 289, NO. 29, pp. 20377–20385, July 18, 2014


# NCLX Protein, but Not LETM1, Mediates Mitochondrial $Ca^{2+}$ Extrusion, Thereby Limiting $Ca^{2+}$-induced NAD(P)H Production and Modulating Matrix Redox State*

Received for publication, December 18, 2013, and in revised form, May 12, 2014 Published, JBC Papers in Press, June 4, 2014, DOI 10.1074/jbc.M113.540898

**Umberto De Marchi**[‡§1], **Jaime Santo-Domingo**[‡§], **Cyril Castelbou**[§], **Israel Sekler**[¶], **Andreas Wiederkehr**[‡], **and Nicolas Demaurex**[§2]

*From the* [‡]*Mitochondrial Function, Nestlé Institute of Health Sciences, EPFL Innovation Park, Building G, CH-1015 Lausanne, Switzerland, the* [§]*Department of Cell Physiology and Metabolism, University of Geneva, Rue Michel-Servet, 1, CH-1211 Genève, Switzerland, and the* [¶]*Department of Physiology, Ben-Gurion University of Negev, Beer-Sheva 84105, Israel*

**Background:** Whether mitochondrial $Ca^{2+}$ extrusion is mediated by NCLX (mitochondrial sodium/calcium exchanger) or LETM1 (leucine zipper-EF-hand-containing transmembrane protein 1) and controls matrix redox state is unknown.
**Results:** NCLX, but not LETM1, increases $Ca^{2+}$ extrusion, limits NAD(P)H production, and promotes matrix oxidation.
**Conclusion:** NCLX controls the duration of matrix $Ca^{2+}$ elevations and their impact on redox signaling.
**Significance:** NCLX is a potential target for the treatment of redox-dependent diseases.

**Mitochondria capture and subsequently release $Ca^{2+}$ ions, thereby sensing and shaping cellular $Ca^{2+}$ signals. The $Ca^{2+}$ uniporter MCU mediates $Ca^{2+}$ uptake, whereas NCLX (mitochondrial Na/Ca exchanger) and LETM1 (leucine zipper-EF-hand-containing transmembrane protein 1) were proposed to exchange $Ca^{2+}$ against $Na^+$ or $H^+$, respectively. Here we study the role of these ion exchangers in mitochondrial $Ca^{2+}$ extrusion and in $Ca^{2+}$-metabolic coupling. Both NCLX and LETM1 proteins were expressed in HeLa cells mitochondria. The rate of mitochondrial $Ca^{2+}$ efflux, measured with a genetically encoded indicator during agonist stimulations, increased with the amplitude of mitochondrial $Ca^{2+}$ ($[Ca^{2+}]_{mt}$) elevations. NCLX overexpression enhanced the rates of $Ca^{2+}$ efflux, whereas increasing LETM1 levels had no impact on $Ca^{2+}$ extrusion. The fluorescence of the redox-sensitive probe roGFP increased during $[Ca^{2+}]_{mt}$ elevations, indicating a net reduction of the matrix. This redox response was abolished by NCLX overexpression and restored by the $Na^+/Ca^{2+}$ exchanger inhibitor CGP37157. The $[Ca^{2+}]_{mt}$ elevations were associated with increases in the autofluorescence of NAD(P)H, whose amplitude was strongly reduced by NCLX overexpression, an effect reverted by $Na^+/Ca^{2+}$ exchange inhibition. We conclude that NCLX, but not LETM1, mediates $Ca^{2+}$ extrusion from mitochondria. By controlling the duration of matrix $Ca^{2+}$ elevations, NCLX contributes to the regulation of NAD(P)H production and to the conversion of $Ca^{2+}$ signals into redox changes.**

$Ca^{2+}$ is a versatile intracellular messenger controlling most cellular processes. In order to maintain normal signaling function, tight spatial/temporal control of $Ca^{2+}$ is essential. To achieve such tight regulation, cells are equipped with a number of proteins mediating the transport of $Ca^{2+}$ across the plasma membrane, the endoplasmic reticulum, and the inner mitochondrial membrane (1). Mitochondria contribute to the shaping of $Ca^{2+}$ signals through $Ca^{2+}$ uptake and release (2–9). At the same time, the associated $[Ca^{2+}]_{mt}$[3] transients act as signals to stimulate energy metabolism.

The amplitude and duration of $[Ca^{2+}]_{mt}$ elevations reflect the balance between uptake and release mechanisms (10–13). Uptake is performed by the recently identified mitochondrial $Ca^{2+}$ uniporter (MCU) (14, 15), whose activity is tightly controlled by the regulatory molecules MICU1, MICU2, MCUR1, and EMRE (16–19). The MCU forms a channel with high selectivity but low affinity for $Ca^{2+}$ (10, 20). Despite this low affinity, mitochondria can accumulate large amounts of $Ca^{2+}$ during cell stimulation when exposed to microdomains of high $Ca^{2+}$ concentration (21), forming in the vicinity of intracellular $Ca^{2+}$ release or plasma membrane $Ca^{2+}$ entry channels (22, 23).

Mitochondrial $Ca^{2+}$ uptake activates several $Ca^{2+}$-dependent matrix enzymes that stimulate energy metabolism (24, 25) and ATP synthase-dependent respiration (26). Prolonged (pathological) accumulation of $Ca^{2+}$ in the matrix space can lead to mitochondrial $Ca^{2+}$ overload, followed by mitochondrial permeability transition pore opening (27–29), resulting in the activation of cell death signals (30, 31). To avoid this transition from stimulatory to detrimental effects of $Ca^{2+}$, mitochondria possess two membrane systems to extrude $Ca^{2+}$: the $Na^+/Ca^{2+}$ exchanger and the $H^+/Ca^{2+}$ exchanger (5, 6). Two mitochondrial inner membrane proteins, namely NCLX (32) (sodium/calcium exchanger protein, mitochondrial; or sodium/potassium/calcium exchanger 6, mitochondrial; or solute carrier family 24 member 6) and LETM1 (33) (LETM1 and EF-

* This work was supported by Swiss National Foundation Grant 310030B_133126 (to N. D.).

[1] To whom correspondence may be addressed: Mitochondrial Function, Nestlé Institute of Health Sciences, EPFL Innovation Park, Bldg. G, CH-1015 Lausanne, Switzerland. Tel.: 41-21-632-6122; E-mail: Umberto.DeMarchi@rd.nestle.com.

[2] To whom correspondence may be addressed: Dept. of Cell Physiology and Metabolism, University of Geneva, Rue Michel-Servet 1, CH-1211 Geneva 4, Switzerland. Tel.: 41-22-379-5399; Fax: 41-22-379-5338; E-mail: Nicolas.Demaurex@unige.ch.

[3] The abbreviations used are: $[Ca^{2+}]_{mt}$, mitochondrial $[Ca^{2+}]$; MCU, mitochondrial $Ca^{2+}$ uniporter; ROS, reactive oxygen species.

hand domain-containing protein 1, mitochondrial; or leucine zipper-EF-hand-containing transmembrane protein 1) have been recently proposed to exchange $Ca^{2+}$ against $Na^+$ or $H^+$, respectively. Functional analysis strongly suggests that NCLX is a mitochondrial $Na^+/Ca^{2+}$ exchanger because overexpression of this protein enhances mitochondrial $Ca^{2+}$ efflux, whereas its knockdown diminishes $Ca^{2+}$ extrusion. Furthermore, pharmacological inhibition of mitochondrial $Ca^{2+}$ efflux with the benzothiazepine derivative CGP37157 completely blocks NCLX-dependent $Ca^{2+}$ export. LETM1 was proposed to be a high affinity mitochondrial $Ca^{2+}/H^+$ exchanger (33, 34) able to drive both extrusion and uptake of $Ca^{2+}$ into energized mitochondria at submicromolar $Ca^{2+}$ concentrations. Previous studies, however, indicated that LETM1 mediates mitochondrial $K^+/H^+$ exchange (35, 36), and the contribution of LETM1 to mitochondrial $Ca^{2+}$ transport is not yet firmly established (37). One factor hindering studies of mitochondrial $Ca^{2+}$ extrusion is the large variability in the kinetics of mitochondrial $Ca^{2+}$ efflux between cells during physiological stimuli. Perfectly detailed protocols have been available from the 1970s, for the quantitative analysis of $Ca^{2+}$ efflux, and an elegant series of studies carried out by Carafoli and co-workers (38, 39) on isolated mitochondria examined the pathway and mechanism of $Ca^{2+}$ release. Nevertheless, protocols enabling the quantitative analysis of mitochondrial $Ca^{2+}$ efflux in live cells, where the analysis of this process is complicated by cell-to-cell variability, are lacking.

The transient matrix $Ca^{2+}$ elevations have several effects on mitochondrial function. The energetic redox balance in particular is a primary target of the mitochondrial $Ca^{2+}$ homeostasis (40), with strong impact on metabolic regulation (41) and human health (42). Inside the organelle, $Ca^{2+}$ activates oxidative metabolism and respiration. In addition, $[Ca^{2+}]_{mt}$ elevations can have several and sometimes opposing effects on the redox balance. On the one hand, $[Ca^{2+}]_{mt}$ elevations activate $Ca^{2+}$-dependent dehydrogenases, accelerating NADH production (25). As a result, the ratio of the redox couple NAD(P)H/NAD(P) will increase (43–47). On the other hand, $[Ca^{2+}]_{mt}$ elevations accelerate respiration. This will increase the associated formation of reactive oxygen species (ROS) (48, 49), with a net oxidizing effect in the matrix space.

Here we have studied the role of NCLX and LETM1 in the export of $Ca^{2+}$ from the mitochondrial matrix space. In order to properly describe mitochondrial $Ca^{2+}$ export kinetics, we have applied a biparametric single-cell analysis. This novel approach allowed us to determine the contribution of different $Ca^{2+}$ export systems in an amplitude-dependent manner. Furthermore, we have assessed the importance of $Ca^{2+}$ extrusion kinetics in the regulation of oxidative metabolism and in the control of the mitochondrial redox state.

## EXPERIMENTAL PROCEDURES

*Reagents*—Histamine, dithiothreitol (DTT), $H_2O_2$, and rotenone were obtained from Sigma, and CGP37157 was from Calbiochem. Preparation of NCLX-encoding plasmid was described previously (32). The 4mtD3cpv construct (50) was provided by Drs. Amy Palmer and Roger Tsien (University of California, San Diego). The mitochondrial redox indicator roGFP1 (51) was provided by Dr. S. James Remington (University of Oregon). The LETM1-encoding plasmid (35) was provided by Dr. Luca Scorrano (University of Geneva). The mitochondrial pH sensor mitoSypHer was described previously (52).

*Cell Culture and Transfection*—Minimal essential medium (DMEM), fetal calf serum, penicillin, streptomycin, and Lipofectamine 2000 transfection reagent were from Invitrogen. HeLa cells were cultured in DMEM + 10% fetal calf serum, as described previously (53). For overexpression experiments, cells were plated on 25-mm diameter glass coverslips and co-transfected with the appropriate construct (NCLX, LETM1, or pcDNA3; 1 $\mu$g/ml) and a construct encoding a probe for mitochondrial $Ca^{2+}$ (4mD3cpv), redox status (roGFP1), or mitochondrial pH (mitoSypHer) at a 2:1 ratio, using Lipofectamine 2000 transfection reagent. All experiments were performed 2 days after transfection.

*Cell Lysis, mitochondrial Isolation, and Western Blotting*—Whole cells were lysed for 30 min on ice in lysis buffer (25 mM Tris-HCl, pH 7.6, 150 mM NaCl, 1% Nonidet P-40, 1% sodium deoxycholate, 0.1% SDS), supplemented with protease inhibitors (Roche Applied Science). The lysate was centrifuged at 14,000 $\times$ *g* for 20 min, and the protein content of the supernatant was determined using a BCA protein assay (Pierce). Mitochondrial fractions were obtained by differential centrifugation as reported previously (54). Cell lysates or isolated mitochondria (50 $\mu$g) were separated on SDS-polyacrylamide gels. For immunoblotting, proteins were transferred onto nitrocellulose membrane and probed with the following antibodies: anti-NCLX (Santa Cruz Biotechnology, Inc., sc-1611921), anti-LETM1 (Santa Cruz Biotechnology, sc-271234), anti-Tom20 (Santa Cruz Biotechnology, sc-11415), and anti-tubulin (Sigma, T9026). Horseradish peroxidase-conjugated secondary antibodies (Amersham Biosciences) were used and detected by chemiluminescence (Amersham Biosciences).

*Mitochondrial $Ca^{2+}$ Measurements*—Experiments were performed in HEPES buffer containing 140 mM NaCl, 5 mM KCl, 1 mM $MgCl_2$, 2 mM $CaCl_2$, 20 mM Hepes, 10 mM glucose, pH 7.4, with NaOH at 37 °C. Glass coverslips were inserted in a thermostatic chamber (Harvard Apparatus, Holliston, MA), and solutions were changed by hand. Cells were imaged on an Axiovert s100 TV using a $\times$40, 1.3 numeric aperture oil immersion objective (Carl Zeiss AG, Feldbach, Switzerland) and a cooled, 16-bit CCD back-illuminated frame transfer MicroMax camera (Roper Scientific, Trenton, NJ). $[Ca^{2+}]_{mt}$ was measured with the genetically encoded 4mtD3cpv sensor. Cells were excited at 430 nm through a 455DRLP dichroic and alternately imaged with 480AF30 and 535DF25 emission filters (Omega Optical). Images were acquired every 2 s. Fluorescence ratios were calculated in MetaFluor 6.3 (Universal Imaging) and analyzed in Excel (Microsoft) and GraphPad Prism 5 (GraphPad). $[Ca^{2+}]_{mt}$ was calculated *in situ* in semipermeabilized cells as described previously (55) from 4mtD3cpv ratios (*R*) using the following equation.

$$[Ca^{2+}] = [K' d^n \times (R - R_{min})/(R_{max} - R)]^{1/n} \quad \text{(Eq. 1)}$$

$R_{min}$ was obtained by treating the cells with 1 mM EGTA along with 10 $\mu$M ionomycin, and $R_{max}$ was obtained by treating the

cells with 10 μM ionomycin and 10 mM $Ca^{2+}$. The maximal $Ca^{2+}$ efflux rates were calculated by performing a first order derivative on the data obtained during the first minute of the decay phase of the $Ca^{2+}$ response.

*Mitochondrial Matrix pH Measurements in Permeabilized Cells*—Ratiometric measurements of the mitochondrial pH were performed on the same instrument as for $[Ca^{2+}]_{mt}$ measurements, using the mitochondrial targeted sensor mito-SypHer. Cells were alternately excited at 420 and 490 nm through a 505DCXR dichroic filter and imaged with a 535DF25 band pass filter (Omega Optical) as described previously (52). Images were acquired every 5 s. MitoSypHer-expressing HeLa cells were permeabilized on the microscope with a 1-min exposure to digitonin (100 μM) in $Ca^{2+}$-free intracellular buffer, containing 235 mM sucrose, 20 mM HEPES, 5 mM succinic acid, 1 mM EGTA, adjusted to pH 7.4 with *N*-methyl-D-glucamine. After digitonin washout, cells were kept in intracellular buffer for 10 min, before $K^+$-driven $H^+$ extrusion was evoked by changing the intracellular solution with a $K^+$-gluconate solution containing 50 mM potassium gluconate, 135 mM sucrose, 20 mM HEPES, 5 mM succinic acid, 1 mm EGTA, adjusted to pH 7.4 with *N*-methyl-D-glucamine. The ratiometric 490/420 signals were normalized to the basal level (set to 1), and the amplitude of $K^+$-evoked ΔpH was calculated.

*Mitochondrial Redox State Measurements*—Ratiometric measurements of the mitochondrial redox state were performed by using the same instrument as described for $[Ca^{2+}]_{mt}$ measurements, using the mitochondrially targeted, genetically encoded sensor roGFP1. Cells were excited at 410 and 480 nm, and emission was collected at 535 nm (535DF45, Omega Optical) through a 505DCXR (Omega Optical) dichroic mirror. Images were acquired every 2 s. The 480/410 fluorescence ratios were normalized to both the minimum of fluorescence (obtained after the addition of 1 mM $H_2O_2$) and the maximum (obtained after the addition of 10 mM DTT).

*NAD(P)H Measurements*—Cells were allowed to adhere to glass bottom dishes (MatTek, Ashland, MA) for 2 days, and experiments were performed in the Hepes buffer solution as described above. A laser-scanning confocal microscope (Leica TCS SP5 II MP, Manheim, Germany) with a HCX IRAPO L ×25/0.95 water objective was utilized to monitor NAD(P)H autofluorescence at 37 °C (Life Imaging Services). Laser scans at 727 nm (IR Laser Chameleon ultra, Coherent) were used for two-photon NAD(P)H excitation. Each 512 × 512-pixel image represents an average of 16 scans taken with a resonant scanner at 8000 Hz. NAD(P)H emission was collected at 445–495-nm wavelength every 20 s. The excitation power of the laser was set to avoid cellular photodamage. Data were processed with LAS AF software (Leica) and analyzed in Excel (Microsoft) and GraphPad Prism 5 (GraphPad). In order to normalize the NAD(P)H responses, each experiment was concluded by adding the complex I inhibitor rotenone, which results in the accumulation of NAD(P)H (autofluorescence close to maximal), followed by peroxide, where the autofluorescence is almost completely lost (minimal value). Fluorescence intensity data were normalized to both rotenone addition (equal to 1) and minimal value (hydrogen peroxide = 0). Change in fluorescence (ΔNAD(P)H) were calculated as the difference between the effect of histamine after reaching a plateau and the baseline value.

*Statistics*—The significance of differences between means was established using Student's *t* test for unpaired samples (*, $p < 0.05$; **, $p < 0.01$; ***, $p < 0.001$; *NS*, not significant).

## RESULTS

*Biparametric Analysis of Mitochondrial $Ca^{2+}$ Extrusion Rates*—To assess the kinetics of $Ca^{2+}$ efflux from mitochondria, we measured $[Ca^{2+}]_{mt}$ changes evoked by physiological agonists in HeLa cells with the mitochondrially targeted $Ca^{2+}$ sensor 4mtD3cpv. Application of the endoplasmic reticulum $Ca^{2+}$-mobilizing agonist histamine rapidly increased $[Ca^{2+}]_{mt}$ to ~2.5 μM (Fig. 1*A*), but the amplitude and kinetics of the elevations were highly variable, even between cells of the same clonal population recorded simultaneously (Fig. 1*B*). Importantly, the $Ca^{2+}$ efflux kinetics increased together with the amplitude of $[Ca^{2+}]_{mt}$ elevations, with large elevations followed by rapid $Ca^{2+}$ efflux and small elevations followed by a sustained plateau. This heterogeneity prompted us to perform a biparametric analysis and to measure both the maximal rates of $Ca^{2+}$ extrusion and the amplitude of the $[Ca^{2+}]_{mt}$ response (Fig. 1*C*). The efflux rates were then expressed as a function of the corresponding signal amplitude by aggregating the data over defined ranges of $[Ca^{2+}]_{mt}$, which allowed us to model the $[Ca^{2+}]_{mt}$-$Ca^{2+}$ efflux relationship by an exponential fit (Fig. 1*D*). This approach enabled us to include all of the cells recorded while preserving the complexity of the underlying biological process.

*NCLX Levels but Not LETM1 Levels Modulate Matrix $Ca^{2+}$ Extrusion at High $[Ca^{2+}]_{mt}$*—We then assessed the contribution of NCLX and LETM1 to mitochondrial $Ca^{2+}$ extrusion. Consistent with their proposed roles as mitochondrial $Ca^{2+}/Na^+$ and $Ca^{2+}/H^+$ exchangers, both proteins were strongly enriched together with the outer mitochondrial membrane protein TOM20 in mitochondrial fractions from HeLa cells (Fig. 2*A*). NCLX overexpression (32) did not alter the average amplitude of the $[Ca^{2+}]_{mt}$ elevations evoked by histamine (not shown) but accelerated the kinetics of mitochondrial $Ca^{2+}$ efflux (Fig. 2*B*). The biparametric analysis revealed that NCLX accelerated $Ca^{2+}$ efflux exclusively in cells undergoing large $[Ca^{2+}]_{mt}$ elevations (Fig. 3*C*). Separate analysis of cells exhibiting small ($\Delta R/R_0 \leq 0.3$) and large ($\Delta R/R_0 > 0.3$) elevations confirmed that NCLX enhanced mitochondrial $Ca^{2+}$ extrusion only in cells experiencing large $[Ca^{2+}]_{mt}$ elevations (Fig. 2*D*). CGP37157, an inhibitor of the mitochondrial $Na^+/Ca^{2+}$ exchanger, almost completely prevented $Ca^{2+}$ efflux, regardless of NCLX overexpression (Fig. 2, *B–D*). The inhibition was reversible (not shown) and particularly evident in cells undergoing large $[Ca^{2+}]_{mt}$ elevations (Fig. 2*D*). We then tested whether the proposed $Ca^{2+}/H^+$ exchanger LETM1 could affect $Ca^{2+}$ efflux, possibly over a range of $[Ca^{2+}]_{mt}$ distinct from NCLX. Overexpression of LETM1 (35) was validated by Western blot, and the function of the overexpressed protein was tested in permeabilized cells (Fig. 3, *A* and *B*). LETM1 was originally identified as a key element of mitochondrial volume homeostasis through regulation of $K^+/H^+$ exchange (37). In our hands, overexpression of LETM1 increased $K^+$-driven

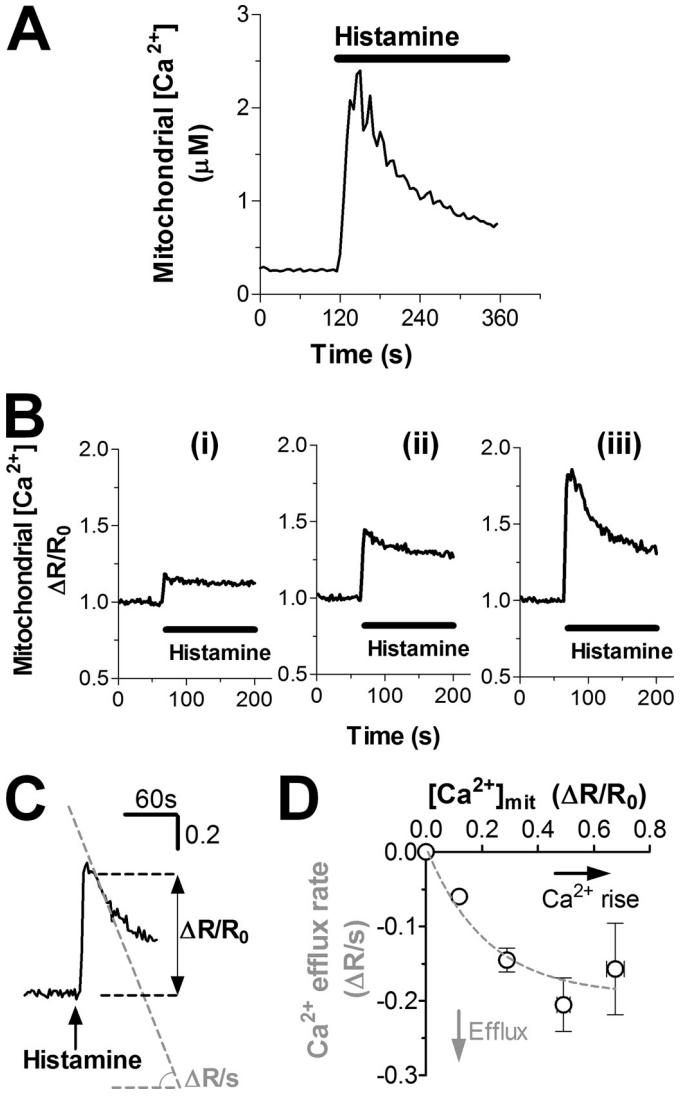


FIGURE 1. **Biparametric analysis of mitochondrial $Ca^{2+}$ extrusion rates.** HeLa cells were transiently transfected with the mitochondrial $Ca^{2+}$ probe 4mtD3cpv. *A*, typical $[Ca^{2+}]_{mt}$ response evoked by histamine (50 $\mu$M) in HeLa cells. The averaged peak amplitude of 26 cells ($n = 4$ experiments) is 2.5 ± 0.79 $\mu$M. *B*, original recordings of three HeLa cells (*i*, *ii*, and *iii*) from the same coverslip stimulated with 100 $\mu$M histamine. *C*, measurements of maximal mitochondrial $Ca^{2+}$ efflux rates ($\Delta R/s$) and $[Ca^{2+}]_{mt}$ signal amplitude ($\Delta R/R_0$). *D*, $Ca^{2+}$ efflux rates as a function of the $[Ca^{2+}]_{mt}$ signal amplitude. Data from 64 cells ($n = 10$) were aggregated for different ranges of $[Ca^{2+}]_{mt}$ values and expressed as a function of $[Ca^{2+}]_{mt}$. The *horizontal error bars* are the mean ± S.E. (*error bars*) of the $Ca^{2+}$ signal amplitude. A *dotted line* shows the exponential regression through the data.

matrix proton extrusion (Fig. 3*B*), consistent with the overexpression of a functional $K^+/H^+$ exchanger (Fig. 3*B*). On the other hand, LETM1 did not alter $Ca^{2+}$ efflux rates, regardless of the amplitude of $[Ca^{2+}]_{mt}$ elevations (Fig. 3, *C–E*). These data demonstrate that NCLX but not LETM1 levels limit the rates of $Ca^{2+}$ extrusion from mitochondria, an effect most apparent during large $[Ca^{2+}]_{mt}$ elevations in HeLa cells that endogenously express both exchangers.

*NCLX Levels Modulate the Mitochondrial Redox State during Stimulation*—Through its impact on the duration of $[Ca^{2+}]_{mt}$ elevations, NCLX may affect intramitochondrial $Ca^{2+}$-dependent processes and alter the mitochondrial redox status. To test this possibility, we measured the mitochondrial redox state using the genetically encoded redox-sensitive probe roGFP1 (51), which contains engineered surface cysteine groups positioned to reversibly form disulfide bonds. Expression of matrix-targeted roGFP1 labeled mitochondria (Fig. 4*A*), and the fluorescence signal increased during histamine application, indicating a more reduced state (Fig. 4*B*). To compare redox responses, we determined the full signal range of the probe in each experiment using peroxide to oxidize roGFP1 followed by reduction of the probe with dithiothreitol (Fig. 4*B*). NCLX overexpression did not affect the basal redox state prior to histamine addition (Fig. 4*C*) but completely prevented the histamine-induced redox changes (Fig. 4, *B* and *D*), an effect that was partially reverted by CGP37157 (Fig. 4, *B* and *D*). These results demonstrate that NCLX levels regulate the mitochondrial redox state, probably by altering the duration of $[Ca^{2+}]_{mt}$ elevations.

*NCLX Levels Limit Histamine-induced Mitochondrial NAD(P)H Production*—The observed net reduction of mitochondrial matrix redox state led us to speculate that NCLX, via its effect on matrix $Ca^{2+}$, might regulate $Ca^{2+}$-dependent matrix dehydrogenases. To test this possibility, we measured changes in NAD(P)H autofluorescence by two-photon microscopy. Histamine application increased the NAD(P)H autofluorescence of HeLa cells (Fig. 5*A*), indicating a net reduction of $NAD(P)^+$ to NAD(P)H, confirming earlier studies (56, 57). To compare NAD(P)H responses, we calibrated each recording by adding the complex I inhibitor rotenone to promote maximal accumulation of NAD(P)H, followed by peroxide to decrease the autofluorescence to the minimal value. NCLX overexpression did not affect the basal autofluorescence levels of HeLa cells (Fig. 5*B*) but severely blunted histamine-induced NAD(P)H formation, by 73%, an effect fully prevented by CGP37157 (Fig. 5*C*). We conclude that NCLX levels are critical for the $[Ca^{2+}]_{mt}$-dependent regulation of the mitochondrial oxidative metabolism.

## DISCUSSION

Mitochondria sense and shape $Ca^{2+}$ signals during cell stimulation (2–6, 58) via their ability to take up and subsequently release $Ca^{2+}$ ions. $Ca^{2+}$ sequestration in the mitochondrial matrix contributes to the buffering of cytosolic $Ca^{2+}$ elevations and serves as a signal that activates mitochondrial $Ca^{2+}$-dependent processes (24, 25). In contrast, prolonged accumulation of $Ca^{2+}$ in the matrix triggers mitochondria-induced cell death (28, 31, 58). Here, we assessed the contribution of the two ion exchangers NCLX and LETM1 in the kinetics of mitochondrial $Ca^{2+}$ extrusion and in the control of the matrix redox state.

The proteins that transport $Ca^{2+}$ across the mitochondrial inner membrane were recently identified, and most efforts are currently devoted to defining the mechanism of mitochondrial $Ca^{2+}$ uptake (14, 15, 21–23, 59, 60). However, the extrusion process is equally critical to achieve mitochondrial $Ca^{2+}$-dependent signaling without triggering cell death. Here, we demonstrate that the rates of mitochondrial $Ca^{2+}$ extrusion are related to the $[Ca^{2+}]_{mt}$ amplitude, with high rates of $Ca^{2+}$ efflux following large elevations and very slow rates following small elevations. This amplitude-dependent control of mitochondrial $Ca^{2+}$ export probably serves to maintain $[Ca^{2+}]_{mt}$ in

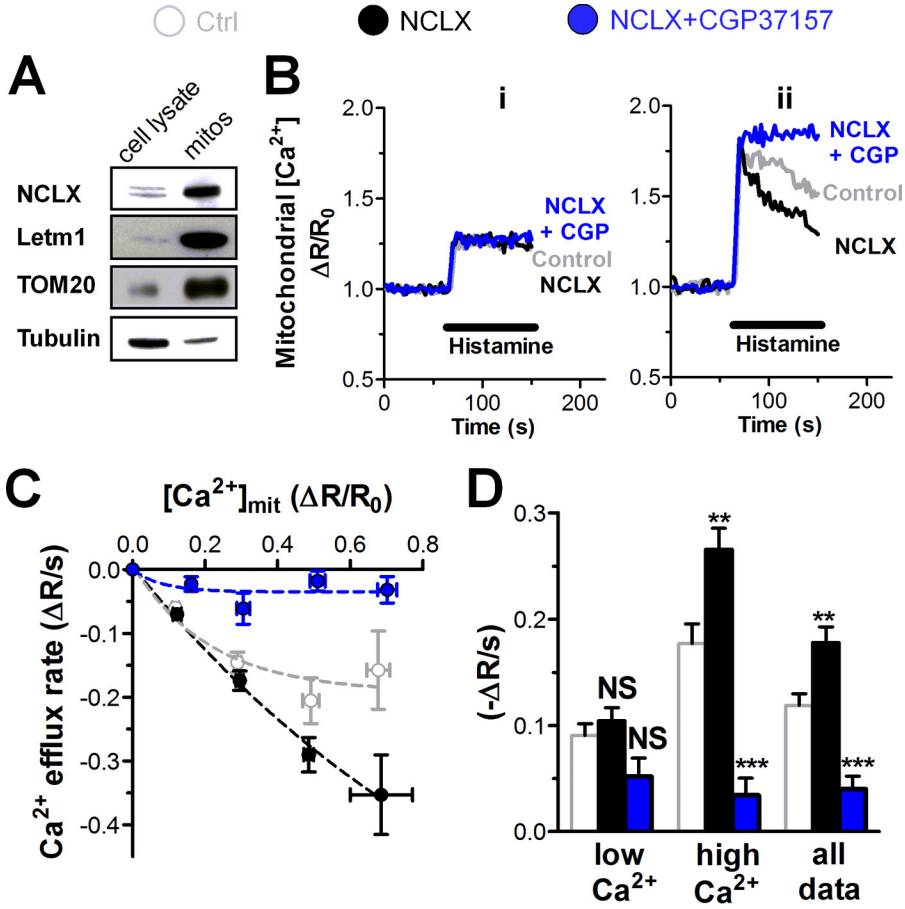


FIGURE 2. **Expression of NCLX enhances mitochondrial $Ca^{2+}$ efflux.** *A*, Western blot showing NCLX and LETM1 immunoreactivity in HeLa cell lysates and mitochondrial fractions (50 $\mu$g of protein each). *B–D*, effect of NCLX expression on mitochondrial $Ca^{2+}$ extrusion. HeLa cells were co-transfected with 4mtD3cpv and an empty vector (*Ctrl*) or NCLX construct (*NCLX*) for 48 h. *B*, original recordings of HeLa cells exposed to histamine (100 $\mu$M). Cells were preincubated for 2 min with 10 $\mu$M CGP37157 (*blue trace*) or HEPES-buffered solution before histamine application. Typical responses for cells with low (*i*; $\Delta R/R \leq 0.3$) and high (*ii*; $\Delta R/R > 0.3$) $[Ca^{2+}]_{mt}$ elevations are shown. *C*, mitochondrial $Ca^{2+}$ efflux rates ($\Delta R/s$) as a function of the $[Ca^{2+}]_{mt}$ signal amplitude measured in control (*white*) and NCLX-overexpressing cells without (*black*) or with 10 $\mu$M CGP37157 (*blue*). *Dotted lines*, exponential regression through the data. *D*, statistical evaluation of the data shown in *C*, showing responses aggregated for all cells (all) or for cells with low ($\Delta R/R \leq 0.3$) and high ($\Delta R/R > 0.3$) $[Ca^{2+}]_{mt}$ elevations. Data are mean ± S.E. (*error bars*) of 64 ($n = 10$), 68 ($n = 10$), and 28 cells ($n = 3$) for control (*white*), NCLX (*black*), and NCLX + CGP37157 (*blue*). **, $p < 0.01$; ***, $p < 0.001$; *NS*, not significant.

a range that is sufficient to activate mitochondrial metabolism (24–26) without reaching the levels that could initiate apoptosis. Our observation that $Ca^{2+}$ extrusion is minimal at low $[Ca^{2+}]_{mt}$ and maximal when mitochondria experience $Ca^{2+}$ signals of large amplitude therefore suggests that the $Ca^{2+}$ extrusion system is tuned to avoid long lasting $[Ca^{2+}]_{mt}$ elevations that can trigger cell death by promoting $Ca^{2+}$-dependent mitochondrial permeability transition pore opening (28, 31). The nature of this $[Ca^{2+}]_{mt}$-sensing mechanism is not known, but several studies suggest the existence of regulatory mechanisms controlling mitochondrial $Ca^{2+}$ export kinetics via direct or indirect interactions with the mitochondrial $Na^+/Ca^{2+}$ exchanger. The protein kinases PKC (61) and PINK1 (62) were reported to modulate the activity of this ion exchanger, and the stomatin-like protein SLP-2, which localizes to the inner mitochondrial membrane, was shown to inhibit mitochondrial $Na^+/Ca^{2+}$ exchange (63). Direct regulation of the exchanger by $Ca^{2+}$ cannot be excluded, but NCLX does not share the hallmark $Ca^{2+}$ regulatory site of plasma membrane $Na^+/Ca^{2+}$ exchange proteins (64).

The $[Ca^{2+}]_{mt}$ dependence of the $Ca^{2+}$ extrusion system, combined with the large cellular variability in the amplitude of $[Ca^{2+}]_{mt}$ responses, prompted us to express $Ca^{2+}$ efflux rates as a function of the $[Ca^{2+}]_{mt}$ amplitude to assess how molecular and pharmacological manipulations alter mitochondrial $Ca^{2+}$ efflux. Using this biparametric analysis, we found that NCLX levels are rate-limiting for mitochondrial $Ca^{2+}$ export during physiological stimulations, whereas LETM1 levels are inconsequential. This confirms earlier studies on NCLX (32) and casts doubt as to the $Ca^{2+}$ exchanger function of LETM1, which remains to be clarified (37). Although mitochondrial $Ca^{2+}$ extrusion is mainly mediated by exchangers (5, 10, 39), the permeability transition pore (27, 29, 30) may contribute to $Ca^{2+}$ release through fast and reversible opening of the channel (65). It would be interesting to test the contribution of the permeability transition pore under physiological conditions using the biparametric analysis presented here.

Given the strong impact of NCLX on mitochondrial $Ca^{2+}$ extrusion kinetics, we further investigated its role in the regulation of mitochondrial oxidative metabolism and redox state.

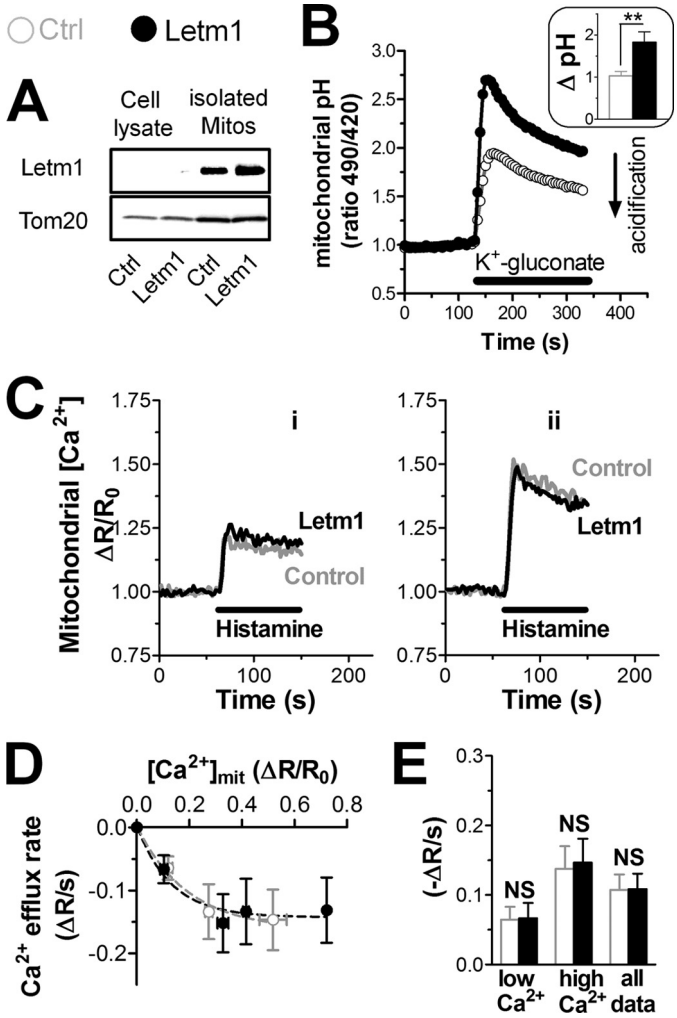


FIGURE 3. **Expression of LETM1 does not alter mitochondrial $Ca^{2+}$ efflux.** Cells were transfected as in Fig. 2 with an empty vector (*Ctrl*) or a LETM1 construct (*Letm1*). *A*, Western blots showing LETM1 immunoreactivity in HeLa cell lysates and in isolated mitochondria (50 $\mu$g of protein each). *B*, effect of LETM1 overexpression on $K^+$-driven mitochondrial proton extrusion in permeabilized cells. HeLa cells were co-transfected with the mitochondrial pH sensor mitoSypHer and an empty vector (*Ctrl*) or LETM1 construct (*Letm1*) for 48 h and permeabilized as described under "Experimental Procedures." Traces show the mean matrix pH response evoked by $K^+$-gluconate (50 mM) of 34 ($n = 5$) and 11 ($n = 3$) cells for control and LETM1, respectively. *Inset*, amplitude of matrix alkalinization (Δratio 490/420 (Δ*pH*)) evoked by $K^+$-gluconate. *C*, $[Ca^{2+}]_{mt}$ elevations evoked by 100 $\mu$M histamine, showing typical responses of cells with low (*i*; $\Delta R/R \leq 0.3$) and high (*ii*; $\Delta R/R > 0.3$) $[Ca^{2+}]_{mt}$ elevations. **, $p < 0.01$. *D*, mitochondrial $Ca^{2+}$ efflux rates ($\Delta R/s$) as a function of the $[Ca^{2+}]_{mt}$ signal amplitude. *E*, statistical evaluation of the data shown in *C*, performed as in Fig. 2. Data are mean ± S.E. (*error bars*) of 31 ($n = 5$; *white*) and 30 cells ($n = 5$; *black*) for control and LETM1, respectively. *NS*, not significant.

A complex relationship exists between $[Ca^{2+}]_{mt}$ and matrix redox processes. $Ca^{2+}$ is able to affect the redox state by activating oxidative metabolism but also by influencing the formation of reactive oxygen species. A rise in $[Ca^{2+}]_{mt}$ stimulates several matrix dehydrogenases, which in the presence of substrate are able to increase the NAD(P)H/NAD(P) ratio and, as a consequence, cause a net reduction of the matrix redox state. At the same time as respiration is accelerated, more reactive oxygen species are formed, which should shift redox couples in the direction of oxidation (43–49). Following stimulation with histamine, we observed a net reduction of the redox-sensitive thiol groups of roGFP1 expressed in the mitochondria of HeLa cells

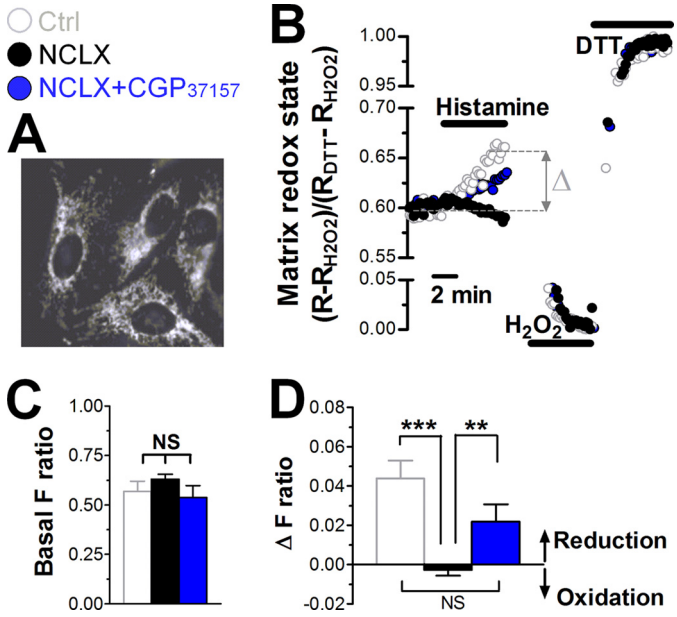


FIGURE 4. **Expression of NCLX modulates mitochondrial matrix redox state during stimulation.** *A*, mitochondrial roGFP fluorescence pattern. *B*, changes in roGFP 480/410 ratio fluorescence evoked by 100 $\mu$M histamine. The fluorescence ratio was normalized to the levels achieved subsequently with 10 mM $H_2O_2$ (ratio = 0) and 100 mM DTT (ratio = 1). *C* and *D*, effect of NCLX expression with and without CGP37157 on the basal roGFP fluorescence (*C*) and on the amplitude of the evoked response (*D*), measured 4 min after histamine addition. Data are mean ± S.E. (*error bars*) of 26 ($n = 4$; *white*), 47 ($n = 7$; *black*), and 13 cells ($n = 4$) for control (*white*), NCLX (*black*), and NCLX + CGP37157 (*blue*). **, $p < 0.01$; ***, $p < 0.001$; *NS*, not significant.

(Fig. 4). Similarly, the histamine-induced $[Ca^{2+}]_{mt}$ rise also increased the NAD(P)H/NAD(P) ratio (Fig. 5). The net redox changes due to histamine-induced $[Ca^{2+}]_{mt}$ elevations appear to be dominated by the activation of $Ca^{2+}$-dependent dehydrogenases. Such redox changes are known to have further downstream effects modulating electron transport, ATP-synthase (66), and matrix enzyme activities (67). Mitochondrial redox signaling has therefore been proposed to be crucial for the regulation of energy metabolism (41, 68). Furthermore, mitochondrial activation and redox changes are linked to the production of ROS at concentrations that impact signaling functions, as shown for glucose-induced insulin secretion (69). Our results establish a direct link between NCLX-mediated mitochondrial $Ca^{2+}$ extrusion and matrix redox state. Redox-dependent processes are therefore sensitive to the regulation of NCLX during stimulus-induced $[Ca^{2+}]_{mt}$ elevations. Given that NCLX shortens the duration of the mitochondrial $Ca^{2+}$ transient (Fig. 2, *B* and *C*) without significantly lowering the amplitude, the effect on the mitochondrial redox state is surprisingly strong (Fig. 4). These results suggest that the fast uptake of $Ca^{2+}$ is not sufficient to modulate the mitochondrial redox state. Instead, $[Ca^{2+}]_{mt}$ elevations must last for a sufficient time to boost NAD(P)H production. This is consistent with previous studies showing that the metabolic decoding of cytosolic $Ca^{2+}$ elevations requires the integration of multiple repetitive elevations (56, 57, 70).

The inhibitor CGP37157 rescued all of the mitochondrial functions affected by NCLX overexpression, indicating that $Na^+/Ca^{2+}$ exchange activity accounts for the changes in oxidative metabolism and redox state. In the presence of the inhibitor, $Ca^{2+}$ extrusion was minimal regardless of NCLX overexpression, whereas

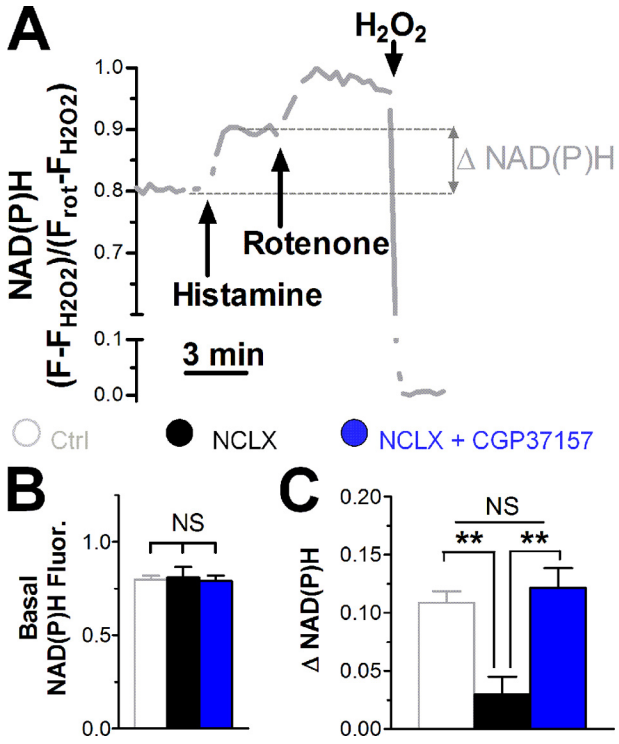


FIGURE 5. **Expression of the NCLX limits histamine-induced NAD(P)H production.** *A*, changes in NAD(P)H autofluorescence evoked by 100 $\mu$M histamine. A trace shows the average of 44 cells from a single experiment, normalized to the maximal and minimal values obtained with 1 $\mu$M rotenone and 1% $H_2O_2$, respectively. *B* and *C*, effect of NCLX expression with and without CGP37157 on basal NAD(P)H autofluorescence (*B*) and on the amplitude of the response evoked by histamine (*C*). Data are the mean ± S.E. of four (205 cells), five (226 cells), and four (146 cells) independent experiments for control (*white*), NCLX (*black*), and NCLX + CGP37157 (*blue*). **, $p < 0.01$; *NS*, not significant.

redox changes and NAD(P)H generation in NCLX-overexpressing cells were restored to control levels (Figs. 4 and 5). Based on the almost complete block of $Ca^{2+}$ extrusion, one could have expected a further reduction of the NAD(P)H/NAD(P) ratio in treated cells and a more reduced state in the matrix than control levels. The sustained $[Ca^{2+}]_{mt}$ elevation evoked by CGP37157, however, is expected to augment not only oxidative metabolism and respiration but also ROS formation, which would oxidize the matrix and decrease the NAD(P)H/NAD(P) ratio. The redox state of CGP37157-treated cells might therefore reflect the balance between accelerated NAD(P)H formation and increased ROS-dependent oxidation.

Our data demonstrate that NCLX plays a key role in cell physiology, providing mechanistic insight into the complex interrelations between $Ca^{2+}$ and redox signaling. These results also provide strong evidence for the importance of mitochondrial $Ca^{2+}$ export in the regulation of the mitochondrial oxidative metabolism. The present work identifies NCLX as a target for the modulation of redox-dependent processes.

*Acknowledgments—We thank Drs. R. Y. Tsien and A. Palmer for the cameleon constructs, Dr. S. J. Remington for the roGFP probe, and Dr. Luca Scorrano for the LETM1 construct. We are grateful to Ariane Widmer for excellent technical assistance and to Sergei Startchik for help with the image analysis. We thank M. Frieden for critical reading of the manuscript.*

## REFERENCES

1. Berridge, M. J., Lipp, P., and Bootman, M. D. (2000) The versatility and universality of calcium signalling. *Nat. Rev. Mol. Cell Biol.* **1,** 11–21
2. Vasington, F. D., and Murphy, J. V. (1962) Ca ion uptake by rat kidney mitochondria and its dependence on respiration and phosphorylation. *J. Biol. Chem.* **237,** 2670–2677
3. Deluca, H. F., and Engstrom, G. W. (1961) Calcium uptake by rat kidney mitochondria. *Proc. Natl. Acad. Sci. U.S.A.* **47,** 1744–1750
4. Lehninger, A. L., Rossi, C. S., and Greenawalt, J. W. (1963) Respiration-dependent accumulation of inorganic phosphate and Ca ions by rat liver mitochondria. *Biochem. Biophys. Res. Commun.* **10,** 444–448
5. Crompton, M., Künzi, M., and Carafoli, E. (1977) The calcium-induced and sodium-induced effluxes of calcium from heart mitochondria. Evidence for a sodium-calcium carrier. *Eur. J. Biochem.* **79,** 549–558
6. Pozzan, T., Bragadin, M., and Azzone, G. F. (1977) Disequilibrium between steady-state $Ca^{2+}$ accumulation ratio and membrane potential in mitochondria. Pathway and role of $Ca^{2+}$ efflux. *Biochemistry* **16,** 5618–5625
7. Szabadkai, G., and Duchen, M. R. (2008) Mitochondria: the hub of cellular $Ca^{2+}$ signaling. *Physiology* **23,** 84–94
8. Demaurex, N., Poburko, D., and Frieden, M. (2009) Regulation of plasma membrane calcium fluxes by mitochondria. *Biochim. Biophys. Acta* **1787,** 1383–1394
9. Pizzo, P., Drago, I., Filadi, R., and Pozzan, T. (2012) Mitochondrial $Ca^{2+}$ homeostasis: mechanism, role, and tissue specificities. *Pflugers Arch.* **464,** 3–17
10. Bernardi, P. (1999) Mitochondrial transport of cations: channels, exchangers, and permeability transition. *Physiol. Rev.* **79,** 1127–1155
11. Gunter, T. E., and Sheu, S. S. (2009) Characteristics and possible functions of mitochondrial $Ca^{2+}$ transport mechanisms. *Biochim. Biophys. Acta* **1787,** 1291–1308
12. Santo-Domingo, J., and Demaurex, N. (2010) Calcium uptake mechanisms of mitochondria. *Biochim. Biophys. Acta* **1797,** 907–912
13. Jean-Quartier, C., Bondarenko, A. I., Alam, M. R., Trenker, M., Waldeck-Weiermair, M., Malli, R., and Graier, W. F. (2012) Studying mitochondrial $Ca^{2+}$ uptake: a revisit. *Mol. Cell Endocrinol.* **353,** 114–127
14. Baughman, J. M., Perocchi, F., Girgis, H. S., Plovanich, M., Belcher-Timme, C. A., Sancak, Y., Bao, X. R., Strittmatter, L., Goldberger, O., Bogorad, R. L., Koteliansky, V., and Mootha, V. K. (2011) Integrative genomics identifies MCU as an essential component of the mitochondrial calcium uniporter. *Nature* **476,** 341–345
15. De Stefani, D., Raffaello, A., Teardo, E., Szabò, I., and Rizzuto, R. (2011) A forty-kilodalton protein of the inner membrane is the mitochondrial calcium uniporter. *Nature* **476,** 336–340
16. Perocchi, F., Gohil, V. M., Girgis, H. S., Bao, X. R., McCombs, J. E., Palmer, A. E., and Mootha, V. K. (2010) MICU1 encodes a mitochondrial EF hand protein required for $Ca^{2+}$ uptake. *Nature* **467,** 291–296
17. Mallilankaraman, K., Cárdenas, C., Doonan, P. J., Chandramoorthy, H. C., Irrinki, K. M., Golenar, T., Csordás, G., Madireddi, P., Yang, J., Muller, M., Miller, R., Kolesar, J. E., Molgó, J., Kaufman, B., Hajnóczky, G., Foskett, J. K., and Madesh, M. (2012) MCUR1 is an essential component of mitochondrial $Ca^{2+}$ uptake that regulates cellular metabolism. *Nat. Cell Biol.* **14,** 1336–1343
18. Mallilankaraman, K., Doonan, P., Cárdenas, C., Chandramoorthy, H. C., Muller, M., Miller, R., Hoffman, N. E., Gandhirajan, R. K., Molgó, J., Birnbaum, M. J., Rothberg, B. S., Mak, D. O., Foskett, J. K., and Madesh, M. (2012) MICU1 is an essential gatekeeper for MCU-mediated mitochondrial $Ca^{2+}$ uptake that regulates cell survival. *Cell* **151,** 630–644
19. Sancak, Y., Markhard, A. L., Kitami, T., Kovács-Bogdán, E., Kamer, K. J., Udeshi, N. D., Carr, S. A., Chaudhuri, D., Clapham, D. E., Li, A. A., Calvo, S. E., Goldberger, O., and Mootha, V. K. (2013) EMRE is an essential component of the mitochondrial calcium uniporter complex. *Science* **342,** 1379–1382
20. Kirichok, Y., Krapivinsky, G., and Clapham, D. E. (2004) The mitochondrial calcium uniporter is a highly selective ion channel. *Nature* **427,** 360–364
21. Giacomello, M., Drago, I., Bortolozzi, M., Scorzeto, M., Gianelle, A., Pizzo,

P., and Pozzan, T. (2010) $Ca^{2+}$ hot spots on the mitochondrial surface are generated by $Ca^{2+}$ mobilization from stores, but not by activation of store-operated $Ca^{2+}$ channels. *Mol. Cell* **38,** 280–290
22. Rizzuto, R., Brini, M., Murgia, M., and Pozzan, T. (1993) Microdomains with high $Ca^{2+}$ close to IP3-sensitive channels that are sensed by neighboring mitochondria. *Science* **262,** 744–747
23. Hoth, M., Fanger, C. M., and Lewis, R. S. (1997) Mitochondrial regulation of store-operated calcium signaling in T lymphocytes. *J. Cell Biol.* **137,** 633–648
24. McCormack, J. G., and Denton, R. M. (1979) The effects of calcium ions and adenine nucleotides on the activity of pig heart 2-oxoglutarate dehydrogenase complex. *Biochem. J.* **180,** 533–544
25. Glancy, B., and Balaban, R. S. (2012) Role of mitochondrial $Ca^{2+}$ in the regulation of cellular energetics. *Biochemistry* **51,** 2959–2973
26. De Marchi, U., Thevenet, J., Hermant, A., Dioum, E., and Wiederkehr, A. (2014) Calcium co-regulates oxidative metabolism and ATP synthase-dependent respiration in pancreatic beta cells. *J. Biol. Chem.* **289,** 9182–9194
27. Zoratti, M., Szabò, I., and De Marchi, U. (2005) Mitochondrial permeability transitions: how many doors to the house? *Biochim. Biophys. Acta* **1706,** 40–52
28. Rasola, A., and Bernardi, P. (2011) Mitochondrial permeability transition in $Ca^{2+}$-dependent apoptosis and necrosis. *Cell Calcium* **50,** 222–233
29. Zoratti, M., De Marchi, U., Biasutto, L., and Szabò, I. (2010) Electrophysiology clarifies the megariddles of the mitochondrial permeability transition pore. *FEBS Lett.* **584,** 1997–2004
30. Rasola, A., and Bernardi, P. (2007) The mitochondrial permeability transition pore and its involvement in cell death and in disease pathogenesis. *Apoptosis* **12,** 815–833
31. Gouriou, Y., Demaurex, N., Bijlenga, P., and De Marchi, U. (2011) Mitochondrial calcium handling during ischemia-induced cell death in neurons. *Biochimie* **93,** 2060–2067
32. Palty, R., Silverman, W. F., Hershfinkel, M., Caporale, T., Sensi, S. L., Parnis, J., Nolte, C., Fishman, D., Shoshan-Barmatz, V., Herrmann, S., Khananshvili, D., and Sekler, I. (2010) NCLX is an essential component of mitochondrial $Na^+/Ca^{2+}$ exchange. *Proc. Natl. Acad. Sci. U.S.A.* **107,** 436–441
33. Jiang, D., Zhao, L., and Clapham, D. E. (2009) Genome-wide RNAi screen identifies Letm1 as a mitochondrial $Ca^{2+}/H^+$ antiporter. *Science* **326,** 144–147
34. Jiang, D., Zhao, L., Clish, C. B., and Clapham, D. E. (2013) Letm1, the mitochondrial $Ca^{2+}/H^+$ antiporter, is essential for normal glucose metabolism and alters brain function in Wolf-Hirschhorn syndrome. *Proc. Natl. Acad. Sci. U.S.A.* **110,** E2249–E2254
35. Dimmer, K. S., Navoni, F., Casarin, A., Trevisson, E., Endele, S., Winterpacht, A., Salviati, L., and Scorrano, L. (2008) LETM1, deleted in Wolf-Hirschhorn syndrome, is required for normal mitochondrial morphology and cellular viability. *Hum. Mol. Genet.* **17,** 201–214
36. Nowikovsky, K., Froschauer, E. M., Zsurka, G., Samaj, J., Reipert, S., Kolisek, M., Wiesenberger, G., and Schweyen, R. J. (2004) The LETM1/YOL027 gene family encodes a factor of the mitochondrial $K^+$ homeostasis with a potential role in the Wolf-Hirschhorn syndrome. *J. Biol. Chem.* **279,** 30307–30315
37. Nowikovsky, K., Pozzan, T., Rizzuto, R., Scorrano, L., and Bernardi, P. (2012) Perspectives on: SGP Symposium on Mitochondrial Physiology and Medicine: the pathophysiology of LETM1. *J. Gen. Physiol.* **139,** 445–454
38. Carafoli, E., Tiozzo, R., Lugli, G., Crovetti, F., and Kratzing, C. (1974) The release of calcium from heart mitochondria by sodium. *J. Mol. Cell. Cardiol.* **6,** 361–371
39. Crompton, M., Moser, R., Lüdi, H., and Carafoli, E. (1978) The interrelations between the transport of sodium and calcium in mitochondria of various mammalian tissues. *Eur. J. Biochem.* **82,** 25–31
40. Liu, T., and O'Rourke, B. (2009) Regulation of mitochondrial $Ca^{2+}$ and its effects on energetics and redox balance in normal and failing heart. *J. Bioenerg. Biomembr.* **41,** 127–132
41. Leloup, C., Casteilla, L., Carrière, A., Galinier, A., Benani, A., Carneiro, L., and Pénicaud, L. (2011) Balancing mitochondrial redox signaling: a key point in metabolic regulation. *Antioxid. Redox Signal.* **14,** 519–530
42. Duchen, M. R., and Szabadkai, G. (2010) Roles of mitochondria in human disease. *Essays Biochem.* **47,** 115–137
43. Duchen, M. R. (1992) $Ca^{2+}$-dependent changes in the mitochondrial energetics in single dissociated mouse sensory neurons. *Biochem. J.* **283,** 41–50
44. Duchen, M. R. (2000) Mitochondria and calcium: from cell signalling to cell death. *J. Physiol.* **529,** 57–68
45. Liu, T., and O'Rourke, B. (2008) Enhancing mitochondrial $Ca^{2+}$ uptake in myocytes from failing hearts restores energy supply and demand matching. *Circ. Res.* **103,** 279–288
46. McCormack, J. G., Halestrap, A. P., and Denton, R. M. (1990) Role of calcium ions in regulation of mammalian intramitochondrial metabolism. *Physiol. Rev.* **70,** 391–425
47. Voronina, S., Sukhomlin, T., Johnson, P. R., Erdemli, G., Petersen, O. H., and Tepikin, A. (2002) Correlation of NADH and $Ca^{2+}$ signals in mouse pancreatic acinar cells. *J. Physiol.* **539,** 41–52
48. Kowaltowski, A. J., de Souza-Pinto, N. C., Castilho, R. F., and Vercesi, A. E. (2009) Mitochondria and reactive oxygen species. *Free Radic. Biol. Med.* **47,** 333–343
49. Brookes, P. S., Yoon, Y., Robotham, J. L., Anders, M. W., and Sheu, S. S. (2004) Calcium, ATP, and ROS: a mitochondrial love-hate triangle. *Am. J. Physiol. Cell Physiol.* **287,** C817–C833
50. Palmer, A. E., Giacomello, M., Kortemme, T., Hires, S. A., Lev-Ram, V., Baker, D., and Tsien, R. Y. (2006) $Ca^{2+}$ indicators based on computationally redesigned calmodulin-peptide pairs. *Chem. Biol.* **13,** 521–530
51. Hanson, G. T., Aggeler, R., Oglesbee, D., Cannon, M., Capaldi, R. A., Tsien, R. Y., and Remington, S. J. (2004) Investigating mitochondrial redox potential with redox-sensitive green fluorescent protein indicators. *J. Biol. Chem.* **279,** 13044–13053
52. Poburko, D., Santo-Domingo, J., and Demaurex, N. (2011) Dynamic regulation of the mitochondrial proton gradient during cytosolic calcium elevations. *J. Biol. Chem.* **286,** 11672–11684
53. Jousset, H., Frieden, M., and Demaurex, N. (2007) STIM1 knockdown reveals that store-operated $Ca^{2+}$ channels located close to sarco/endoplasmic $Ca^{2+}$ ATPases (SERCA) pumps silently refill the endoplasmic reticulum. *J. Biol. Chem.* **282,** 11456–11464
54. De Marchi, U., Campello, S., Szabò, I., Tombola, F., Martinou, J. C., and Zoratti, M. (2004) Bax does not directly participate in the $Ca^{2+}$-induced permeability transition of isolated mitochondria. *J. Biol. Chem.* **279,** 37415–37422
55. Palmer, A. E., and Tsien, R. Y. (2006) Measuring calcium signaling using genetically targetable fluorescent indicators. *Nat. Protoc.* **1,** 1057–1065
56. Pralong, W. F., Spät, A., and Wollheim, C. B. (1994) Dynamic pacing of cell metabolism by intracellular $Ca^{2+}$ transients. *J. Biol. Chem.* **269,** 27310–27314
57. Rizzuto, R., Bastianutto, C., Brini, M., Murgia, M., and Pozzan, T. (1994) Mitochondrial $Ca^{2+}$ homeostasis in intact cells. *J. Cell Biol.* **126,** 1183–1194
58. Rizzuto, R., De Stefani, D., Raffaello, A., and Mammucari, C. (2012) Mitochondria as sensors and regulators of calcium signalling. *Nat. Rev. Mol. Cell Biol.* **13,** 566–578
59. De Marchi, U., Castelbou, C., and Demaurex, N. (2011) Uncoupling protein 3 (UCP3) modulates the activity of sarco/endoplasmic reticulum $Ca^{2+}$-ATPase (SERCA) by decreasing mitochondrial ATP production. *J. Biol. Chem.* **286,** 32533–32541
60. Trenker, M., Malli, R., Fertschai, I., Levak-Frank, S., and Graier, W. F. (2007) Uncoupling proteins 2 and 3 are fundamental for mitochondrial $Ca^{2+}$ uniport. *Nat. Cell Biol.* **9,** 445–452
61. Yang, F., He, X. P., Russell, J., and Lu, B. (2003) $Ca^{2+}$ influx-independent synaptic potentiation mediated by mitochondrial $Na^+$-$Ca^{2+}$ exchanger and protein kinase C. *J. Cell Biol.* **163,** 511–523
62. Gandhi, S., Wood-Kaczmar, A., Yao, Z., Plun-Favreau, H., Deas, E., Klupsch, K., Downward, J., Latchman, D. S., Tabrizi, S. J., Wood, N. W., Duchen, M. R., and Abramov, A. Y. (2009) PINK1-associated Parkinson's disease is caused by neuronal vulnerability to calcium-induced cell death. *Mol. Cell* **33,** 627–638
63. Da Cruz, S., De Marchi, U., Frieden, M., Parone, P. A., Martinou, J. C., and Demaurex, N. (2010) SLP-2 negatively modulates mitochondrial sodium-

calcium exchange. *Cell Calcium* **47,** 11–18
64. Palty, R., Hershfinkel, M., and Sekler, I. (2012) Molecular identity and functional properties of the mitochondrial $Na^+/Ca^{2+}$ exchanger. *J. Biol. Chem.* **287,** 31650–31657
65. Bernardi, P., and von Stockum, S. (2012) The permeability transition pore as a $Ca^{2+}$ release channel: new answers to an old question. *Cell Calcium* **52,** 22–27
66. Wang, S. B., Murray, C. I., Chung, H. S., and Van Eyk, J. E. (2013) Redox regulation of mitochondrial ATP synthase. *Trends Cardiovasc. Med.* **23,** 14–18
67. Morris, B. J. (2013) Seven sirtuins for seven deadly diseases ofaging. *Free Radic. Biol. Med.* **56,** 133–171
68. Nemoto, S., Takeda, K., Yu, Z. X., Ferrans, V. J., and Finkel, T. (2000) Role for mitochondrial oxidants as regulators of cellular metabolism. *Mol. Cell. Biol.* **20,** 7311–7318
69. Leloup, C., Tourrel-Cuzin, C., Magnan, C., Karaca, M., Castel, J., Carneiro, L., Colombani, A. L., Ktorza, A., Casteilla, L., and Pénicaud, L. (2009) Mitochondrial reactive oxygen species are obligatory signals for glucose-induced insulin secretion. *Diabetes* **58,** 673–681
70. Hajnóczky, G., Robb-Gaspers, L. D., Seitz, M. B., and Thomas, A. P. (1995) Decoding of cytosolic calcium oscillations in the mitochondria. *Cell* **82,** 415–424